Solid State Communications, Vol. 73, No. 5, pp. 393–398, 1990.
Printed in Great Britain.

0038–1098/90 \$3.00 + .00
Pergamon Press plc

ELECTRON PARAMAGNETIC RESONANCE OF NICKEL IN SILICON. – I. IDENTIFICATION OF SPECTRUM

L.S. Vlasenko,* Nguyên Tiên Són,** A.B. van Oosten and C.A.J. Ammerlaan

Natuurkundig Laboratorium der Universiteit van Amsterdam, Valckenierstraat 65,
NL-1018 XE Amsterdam, The Netherlands

and

A.A. Lebedev, E.S. Taptygov and V.A. Khramtsov

A.F. Ioffe Physico-Technical Institute, Academy of Sciences of the USSR, 194021 Leningrad, USSR

(*Received* 14 *August* 1989 *by B. Mühlschlegel*)

Results are reported on the paramagnetic resonance spectrum recently identified with the negatively charged state of substitutional nickel in *n*-type silicon. Studies were made on the presence of the spectrum in silicon with different concentrations of phosphorus doping and under various conditions of illumination. The centre has orthorhombic-I symmetry. Its resonance spectrum is described by a spin Hamiltonian with effective spin $J = 1/2$ and an anisotropic *g*-tensor with principal values $g_{[1\,0\,0]} = 2.0163$, $g_{[0\,1\,1]} = 2.0536$ and $g_{[0\,\bar{1}\,1]} = 2.0182$. The hyperfine interaction with two ligand silicon nuclei is described by an approximately $\langle 1\,1\,1 \rangle$ axially symmetric tensor with $A_{\parallel} = 132.5$ MHz and $A_{\perp} = 97.5$ MHz. Diffusion of the magnetic ^{61}Ni isotope leads to the appearance of resolved hyperfine structure in the spectrum. The results demonstrate a similarity of negative substitutional nickel in silicon to the Ni_s^- centre in germanium and to the impurities Pd_s^- and Pt_s^- in silicon.

1. INTRODUCTION

ELECTRON paramagnetic resonance (EPR) studies on transition metals in silicon, initiated some thirty years ago in the extensive investigations of Ludwig and Woodbury [1], have provided detailed information on the electronic structure of these systems. Theoretical calculations on electronic structure were stimulated [2] and models to account for observable properties such as lattice sites, charge state and spin were proposed. For substitutional impurities the Ludwig–Woodbury model [3] describes the impurity as tetrahedrally coordinated with bonding to each of the nearest neighbour silicon atoms. Spin and charge are localised on the transition metal. For the late transition metals in the 3*d*, 4*d* and 5*d* series, i.e. for Ni, Pd and Pt, respectively, the vacancy model was proposed more recently by Watkins [4]. In this model these impurities in their negatively charged state are considered to have a closed d^{10}-shell and to be accommodated in a negative vacancy. The unpaired electron spin and charge are on the bond connecting two silicon atoms, as in the negative vacancy. Bonding to two silicon neighbours has been suggested as an alternative intermediate between the cases of full fourfold or zero coordination [5]. The two silicon bonds accommodate one impurity electron each, leaving one hole in its *d* shell. Obviously, the distribution of spin and charge in the three models is different. Spin and charge can manifest themselves by hyperfine and nuclear quadrupole interactions. Since these can be determined by magnetic resonance such experiments provide basic answers regarding the validity of the models.

The relevant data for palladium and platinum in silicon have been available for many years [6]. Also for nickel, data were reported a long time ago, but only for the interstitial site in silicon [1] and for the substitutional centre in germanium [7]. Just recently, a new EPR spectrum was described which was detected after nickel diffusion into *n*-type Czochralski silicon

---

* Permanent address: A.F. Ioffe Physico-Technical Institute, Academy of Sciences of the USSR, 194021 Leningrad, USSR.

** Permanent address: University of Hanoi, Hanoi, Vietnam.

[8]. The centre was described as ⟨1 1 0⟩ axially symmetric with $g_{\parallel} = 2.0537$ and $g_{\perp} = 2.0173$. A preliminary investigation was made of the appearance of the spectum in materials of different phosphorus dopings and after various illumination treatments. It was concluded that the EPR spectrum is related to negative substitutional nickel.

The present paper reports further studies on this spectrum. A more accurate determination of the symmetry of the centre was obtained by resonance measurements at higher resolution. Hyperfine interactions with nickel, isotope ^{61}Ni, and silicon, isotope ^{29}Si, were resolved. Also the experimental conditions to obtain more intensive EPR signals in samples doped with phosphorus to different levels and after illumination with filtered light were investigated.

2. EXPERIMENTAL

Samples for the present experiments were prepared starting from both float-zoned and Czochralski-grown silicon, doped with phosphorus in the concentration range from 5×10^{14} to $5 \times 10^{16}\,\mathrm{cm}^{-3}$. The introduction of nickel was performed by enclosing the sample electroplated with nickel into a quartz ampoule, which was filled with argon gas to a pressure of 200 mbar. Alternatively, in particular for the dopings with the precious ^{61}Ni isotope, nickel was deposited onto silicon by mechanically rubbing a small grain of the metal on the sample surface. Distribution of nickel through the sample was achieved by diffusion at the temperature of 1200°C for times varying from 4 to 24 h. Fast cooling after diffusion was obtained by quenching the whole ampoule into room temperature oil or water. Typical sample dimensions are $15 \times 1.5 \times 1.5\,\mathrm{mm}^3$.

For measurements of electron paramagnetic resonance a K-band (microwave frequency $\nu \simeq 23$ GHz) superheterodyne spectrometer was used, which was tuned to observe the dispersion of the susceptibility. Sample temperature for observation of EPR was 4.2 K. Samples could be illuminated in the microwave cavity by light from a 100 W incandescent halogen lamp. Light was channelled from the source to the sample through a quartz rod. Different optical filters were used to obtain light with maximum photon energy of 0.52 and 0.75 eV.

3. RESULTS

Samples prepared as described in the previous paragraph revealed the same magnetic resonance spectrum as reported in [8] for X-band ($\nu \simeq 9$ GHz) microwave frequency. In the lower resistivity n-type material ($\varrho \simeq 1\,\Omega\,\mathrm{cm}$) the spectrum due to neutral phosphorus is simultaneously present. Spectra measured at microwave frequency $\nu = 23.50$ GHz and for magnetic field **B** approximately parallel to a crystallographic ⟨0 1 1⟩ direction are shown in Fig. 1. The resonances in the field range from 815 to 835 mT are ascribed to the nickel centre. The splitting between the two resonances labelled $C+D$ is due to a slight misalignment of the sample away from the true ⟨0 1 1⟩ direction. The angular variation of line positions was

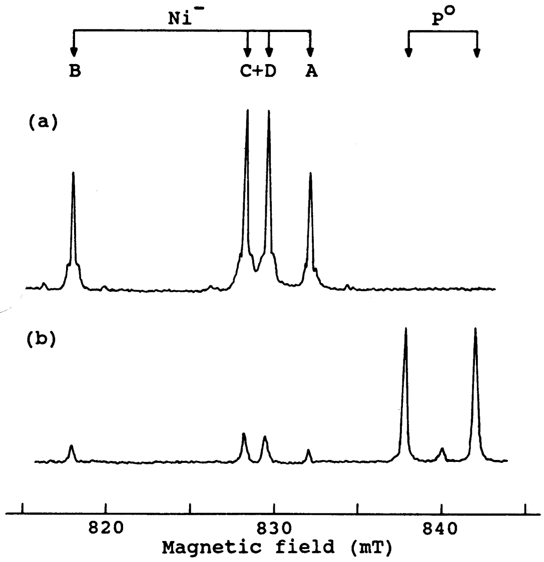

Fig. 1. Electron paramagnetic resonance spectra in nickel and phosphorus doped n-type silicon, observed at temperature 4.2 K for magnetic field **B** nearly parallel to a ⟨0 1 1⟩ crystal direction; (a) phosphorus concentration $\simeq 10^{15}\,\mathrm{cm}^{-3}$, (b) phosphorus concentration $\simeq 5 \times 10^{15}\,\mathrm{cm}^{-3}$.

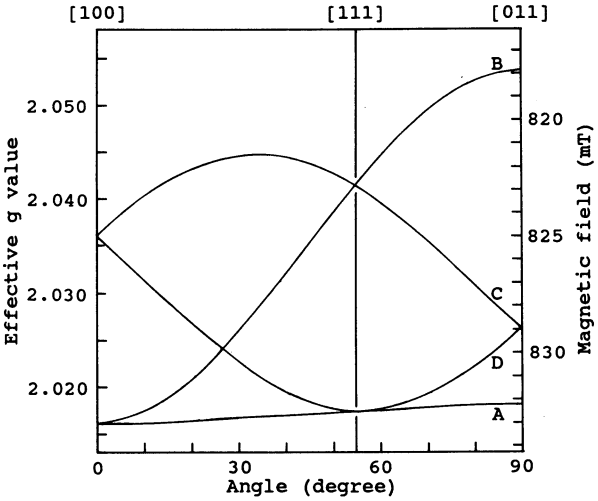

Fig. 2. Angular variation for the Si : Ni spectrum of the effective g-values and resonance fields for rotation of the magnetic field from [1 0 0] to [0 1 1] in the (0 $\bar{1}$ 1) plane.

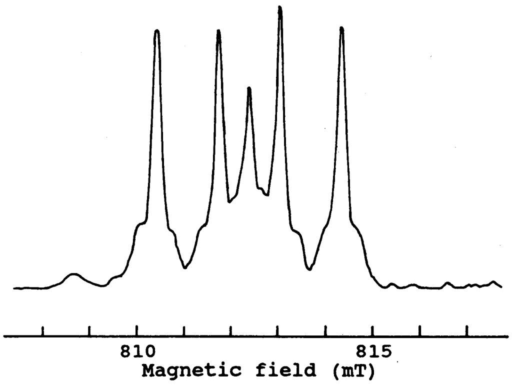

Fig. 3. EPR spectrum for **B** ∥ [0 1 1] near $g_{\text{eff}} = 2.0536$ demonstrating the fourfold hyperfine splitting due to the ^{61}Ni isotope.

measured varying the magnetic field in the $(0\bar{1}1)$ plane. The resulting rotation pattern is shown in Fig. 2. All observed features, such as number of lines, the relative intensities of components $A:B:C:D = 1:1:2:2$, and the pattern style, are unambiguously characteristic for an orthorhombic-I symmetry. Effective g-values g_{eff} were calculated from the resonance condition $h\nu = g_{\text{eff}}\mu_B B$. The principal g-values of the spectrum are $g_{1,\|\langle 100\rangle} = 2.0163$, $g_{2,\|\langle 011\rangle} = 2.0536$ and $g_{3,\|\langle 01\bar{1}\rangle} = 2.0182$.

In order to establish the identity of the centre, nickel enriched to 88.1% in the mass-61 isotope was diffused in samples. This particular stable magnetic isotope has nuclear spin $I = 3/2$. Following such diffusion indeed a hyperfine structure as illustrated in Fig. 3 was observed. For this particular measurement the four strongest lines at equal separations represent the hyperfine splitting according to $m_I = -3/2$, $-1/2$, $+1/2$ and $+3/2$ of ^{61}Ni. The central component corresponds to the 11.9% non-magnetic nickel nuclei. Line intensities are proportional to isotope ratios. The spectrum thus confirms the presence of one nickel atom in the centre. For other magnetic field orientations the spectrum, however, appears to have more complexity. For example Fig. 4 shows the spectrum as observed for **B** ∥ [1 0 0] around $g_{\text{eff}} = 2.036$. The number of lines has increased due to the strong presence of "forbidden" transitions. The full analysis of the angular dependence of the ^{61}Ni hyperfine structure is thereby much more involved and will be discussed in a separate paper [9].

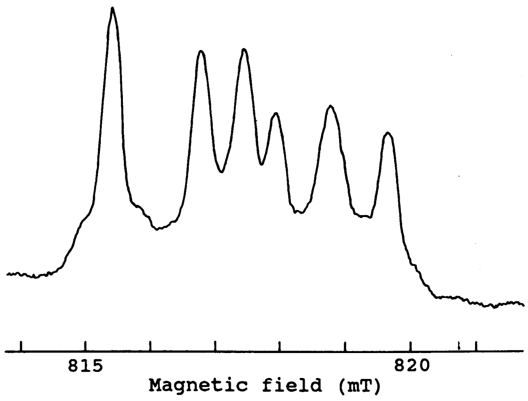

Fig. 4. EPR spectrum for **B** ∥ [1 0 0] near $g_{\text{eff}} = 2.0360$ demonstrating the appearance of forbidden lines in the Si : ^{61}Ni spectrum.

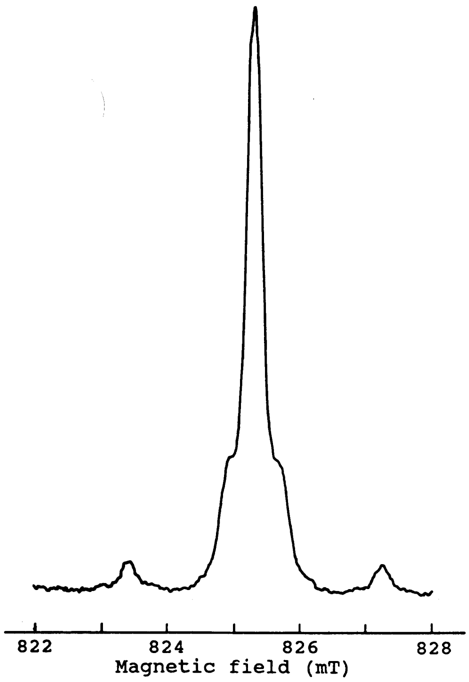

Fig. 5. EPR spectrum of the natural nickel centre for **B** ∥ [1 0 0] showing hyperfine interactions with ^{29}Si nuclei in two shells.

Hyperfine structure due to silicon nuclei near the nickel centre is also apparent in all of the spectra. The magnetic isotope ^{29}Si, with nuclear spin $I = 1/2$, has a natural abundance of 4.7%. Figure 5 shows such interactions with silicon nuclei in two shells. The relative intensity of the outer doublet, with hyperfine splitting of about ± 2 mT, corresponds to the presence of two sites in the shell. The inner doublet, not well resolved from the central line, is associated with a shell containing probably four lattice sites. For the larger hyperfine interaction the angular variation could be followed over the entire range. The result for the centre orientations A and B, which have their $\langle 100\rangle$ principal axis in the magnetic field plane, is shown in Fig. 6. The result reveals a very nearly $\langle 111\rangle$ axial symmetry, with principal values $A_{\|} = 132.5$ and $A_{\perp} = 97.5$ MHz.

To allow for further characterisation of the centre

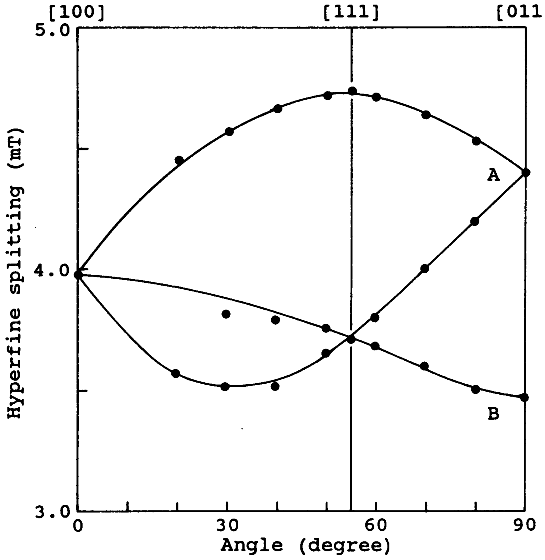

Fig. 6. Angular dependence of the ^{29}Si hyperfine splitting between the two lines in the doublet, in mT, on the EPR orientations A and B.

also the correlation of its intensity with concentration of phosphorus doping was examined. In addition the effect of illumination with white and filtered light was measured. When samples are cooled from room temperature to the measurement temperature without allowing light to reach the sample, the present nickel spectrum is not observed in p-type material. Instead, at 4.2 K the isotropic spectrum with $g = 2.026$ related to Ni_i^+ [1] is detected. The orthorhombic spectrum requires n-type doping for its observation. However, as Fig. 1 illustrates, heavier phosphorus doping in the range above 10^{15} cm^{-3} leads to weaker nickel signals. At the same time the Si : P EPR gives evidence of the presence of the neutral un-ionised phosphorus. For phosphorus concentrations in excess of 10^{16} cm^{-3} the nickel spectrum is absent, only P lines appear.

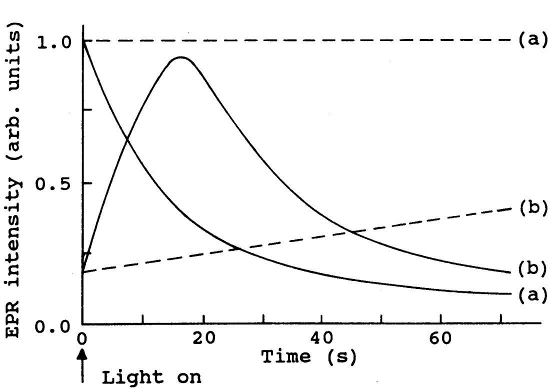

Fig. 7. Intensity of the nickel EPR signal, in arbitrary units, as a function of illumination time with light of $h\nu < 0.52$ eV (dashed curves) or $h\nu < 0.75$ eV (solid curves); (a) sample with phosphorus concentration $n_P \simeq 10^{15}$ cm^{-3}, (b) $n_P \simeq 5 \times 10^{15}$ cm^{-3}.

The behaviour of the nickel spectrum upon illumination is also different depending on the phosphorus doping level. Figure 7 schematically represents some results for light through filters passing maximum energies of 0.52 eV (dashed lines) and 0.75 eV (solid lines). An interesting but complex behaviour was observed in the sample with phosphorus concentration $n_P \simeq 5 \times 10^{15}$ cm^{-3} upon illumination with $h\nu < 0.75$ eV light. An initial enhancement of the spectrum is later followed by its disappearance. For the conditions of our experimental setup the maximum resonance signal is obtained after about 20 s of illumination.

4. DISCUSSION

A multitude of electronic levels, measured by Hall effect and deep level transient spectroscopy (DLTS), has been reported for nickel doped silicon [10–13]. The high diffusivity of nickel favours impurity pairing and other complex formation. Unfortunately, the existing experimental data and models are not well correlated. A definite reliable assignment of electronic levels and charge states to defect configurations is not yet available. However, there still appears to be a common opinion on the existence of a small fraction, $\simeq 0.1\%$, of electrically active nickel. While nickel is assumed to diffuse interstitially, the more stable electrically active species might be on substitutional sites. Amphoteric behaviour, with a donor level at $E_v + 0.17$ eV and an acceptor level at $E_c - 0.41$ eV, has been found frequently. Occasionally double acceptor activity was reported [14]. The intensity dependence of the new nickel related EPR spectrum on the Fermi level, through variation of the phosphorus doping, certainly relates the spectrum to an electrically active centre.

The extreme sensitivity to illumination with light, most easily explained by recharging of the centre, confirms the electrical activity. The behaviour as displayed in Fig. 7 can be tentatively interpreted if it is assumed that the nickel concentration is about 10^{15} cm^{-3}, both in the samples a and b. It is further supposed that nickel can act as a double acceptor, with first ionisation level near midgap and second acceptor level in the upper half of the bandgap near the shallow phosphorus level. In the lightly phosphorus doped sample, $n_P = 10^{15}$ cm^{-3}, all nickel will be present either as Ni^- or Ni^0. Light with $h\nu < 0.52$ eV will have no effect. The more energetic light, $h\nu < 0.75$ eV, will excite electrons from Ni^- centres into the conduction band with their subsequent capture by P^+ centres. This leads to decrease of the nickel spectrum and increase of the phosphorus spec-

Table 1. Principal values of the g-tensors of some related orthorhombic centres

Centre	$g_{[100]}$	$g_{[011]}$	$g_{[0\bar{1}1]}$	Ref.
Ge : Ni$^-$	2.0294	2.0176	2.1128	[7]
Si : Ni$^-$	2.0163	2.0182	2.0536	
Si : Pd$^-$	2.0544	1.9715	1.9190	[6]
Si : Pt$^-$	2.0789	1.4266	1.3867	[6]
Si : V$^-$	2.0038	2.0028	2.0151	[15]

trum, as is observed. In the more strongly doped n-type sample most nickel will be doubly charged. Light of $h\nu < 0.52\,\mathrm{eV}$ can just excite electrons from the highest acceptor level, producing Ni$^-$ and slow enhancement of the spectrum. The same process occurs, but faster, for light $h\nu < 0.75\,\mathrm{eV}$. The initial production of Ni$^-$ centres is then followed by a further, but slower, excitation of electrons producing Ni^0. The concentration of paramagnetic Ni$^-$ then passes through a maximum.

Analysis of the EPR spectrum requires effective spin $J = 1/2$, arising from a single unpaired electron. An odd number of electrons, while neutral nickel supplies an even number, then indicates the presence of a singly ionised centre. With observation of the spectrum only in n-type material, the conclusion of negative charge state is inevitable. The established absence of the spectrum in low resistivity n-type silicon is consistent with the existence of a non-paramagnetic double acceptor state.

Further information on the structure of the centre can be derived by closer consideration of the features of the EPR spectrum. The fourfold splitting observed when the isotope ^{61}Ni is used definitely proves the presence of one nickel atom in the centre. A comparison with the isoelectronic impurities nickel in germanium and palladium and platinum in silicon is suggested. In all these centres the impurity is assumed to be on a substitutional site, in a negatively charged state. Table 1 summarizes the g-tensor constants of the centres. For further comparison the negative vacancy spectrum, Si : V$^-$, is also included. All centres have orthorhombic-I symmetry related to identical distortion modes and similar bonding schemes. The vacancy g-values are close to the free electron value $g = 2.0023$, with little admixture of orbital contributions. The very strong deviations from the pure spin value observed for Pd$^-$ and Pt$^-$, related to d electron orbitals, are absent in the Si : Ni$^-$ case. A fair similarity between the nickel spectra for silicon and germanium is, however, apparent. Also for nickel in germanium, double acceptor nature was concluded on the basis of the experiments.

The electronic distribution is most directly reflected in the hyperfine interactions. Data for the nearest neighbour silicon or germanium atoms of the same centres as discussed above are collected in Table 2. In all cases the hyperfine tensor **A** is nearly $\langle 1\,1\,1\rangle$ axial and is therefore specified by the $A_\parallel$ and $A_\perp$ principal values. For further analysis the standard LCAO approximation, where the wave function is expanded as

$$\psi = \eta(\alpha s_{\mathrm{Si}} + \beta p_{\mathrm{Si}}) \tag{1}$$

is employed. The s part of the wave function, $\eta\alpha$, on the silicon site is related to the isotropic part a of the hyperfine tensor. The p orbitals in the wave function expansion, $\eta\beta$, give the axial component of the interaction tensor.

Briefly, the decomposition of the hyperfine tensor is given by

$$\mathbf{A} = a\mathbf{1} + \mathbf{B}. \tag{2}$$

Relations to the s- and p-type unpaired spin density are

$$a = (2/3)\mu_0 g\mu_B g_N \mu_N \eta^2\alpha^2 |s(0)|^2, \tag{3}$$

$$b = (2/5)\,(1/4\pi)\mu_0 g\mu_B g_N \mu_N \eta^2\beta^2 \langle 1/r^3\rangle_p. \tag{4}$$

Such expressions are more fully discussed for instance in [15]. For numerical analysis the atomic constants

Table 2. Hyperfine data and LCAO coefficients for ligand interactions in some related orthorhombic centres

Centre	$A_\parallel$ (MHz)	$A_\perp$ (MHz)	a (MHz)	b (MHz)	η^2 (%)	α^2 (%)	β^2 (%)	Ref.
Ge : Ni$^-$	59.4	49.5	52.8	3.3	9.1	25	75	[7]
Si : Ni$^-$	132.5	97.5	109.2	11.7	12.6	19	81	
Si : Pd$^-$	150.3	107.1	121.5	14.4	15.2	17	83	[6]
Si : Pt$^-$	114	75	88	13	13.3	14	86	[6]
Si : V$^-$	400.5	333.5	355.8	22.3	27.3	28	72	[15]

$|s(0)|^2$ and $\langle 1/r^3 \rangle_p$ for silicon and germanium are taken from Morton and Preston [16]. Inspection of Table 2, giving the results of the analysis, reveals a close similarity between the spin density on the nearest neighbour atoms of the transition metals. With two atoms in this shell 20 to 30% of an unpaired electron or hole is localised on these neighbours. The predominant distribution of spin density on only two neighbour atoms is consistent with the orthorhombic distortion of the centre. In the vacancy case appreciably higher density of spin on the neighbour sites is found.

In summary, the identification of the EPR spectrum as arising from one nickel atom on a substitutional site with orthorhombic distortion, in a negative charge state, is well supported. The experimental results indicate close similarity of the electronic structure of the transition metal impurities nickel, palladium and platinum in silicon and germanium.

REFERENCES

1. G.W. Ludwig & H.H. Woodbury, *Solid State Phys.* **13,** 223 (1962).
2. A. Zunger, *Solid State Phys.* **39,** 275 (1986).
3. G.W. Ludwig & H.H. Woodbury, *Phys. Rev. Lett.* **5,** 98 (1960).
4. G.D. Watkins, *Physica* **117B & 118B,** 9 (1983).
5. C.A.J. Ammerlaan & A.B. van Oosten, *Physica Scripta* **T25,** 342 (1989).
6. H.H. Woodbury & G.W. Ludwig, *Phys. Rev.* **126,** 466 (1962).
7. G.W. Ludwig & H.H. Woodbury, *Phys. Rev.* **113,** 1014 (1959).
8. L.S. Vlasenko, A.A. Lebedev, E.S. Taptygov & V.A. Khramtsov, *Sov. Tech. Phys. Lett.* **13,** 553 (1987).
9. N.T. Són, A.B. van Oosten & C.A.J. Ammerlaan, to be published.
10. E.R. Weber, *Appl. Phys.* **A30,** 1 (1983).
11. M. Jaraiz, S. Dueñas, J. Vicente, L. Bailón & J. Barbolla, *Solid-State Electronics* **29,** 883 (1986).
12. H. Kitagawa & H. Nakashima, *Phys. Status Solidi (a)* **99,** K49 (1987).
13. H. Lemke, *Phys. Status Solidi (a)* **99,** 205 (1987).
14. W.B. Chua & K. Rose, *J. Appl. Phys.* **41,** 2644 (1970).
15. M. Sprenger, S.H. Muller, E.G. Sieverts & C.A.J. Ammerlaan, *Phys. Rev.* **B35,** 1566 (1987).
16. J.R. Morton & K.F. Preston, *J. Magn. Reson.* **30,** 577 (1978).